

**Comparison of Stop-Jump Muscle Synergies in Amateur Basketball Players with
and without Asymptomatic Patellar Tendon Abnormalities during Simulated
Games**

Dongxu Wang¹, Dong Sun¹, Zhanyi Zhou¹, Fengping Li¹, Xuanzhen Cen¹, Yang
Song², Monèm Jemni³, Yaodong Gu^{1*}

¹Faculty of Sports Science, Ningbo University, Ningbo, China

²Department of Biomedical Engineering, Faculty of Engineering, The Hong Kong
Polytechnic University, Hong Kong, China

³Centre for Mental Health Research in Association, University of Cambridge, Cambridge, UK

*Corresponding author: Yaodong Gu, Faculty of Sports Science, Ningbo University, Ningbo,
China, e-mail address: guyaodong@nbu.edu.cn

Submitted: 3rd September 2024

Accepted: 3rd October 2024

38 **Abstract:**

39 **Purpose:** Asymptomatic patellar tendon abnormality (APTA) is considered a precursor
40 to patellar tendinopathy (PT), but its pathogenesis remains unclear, especially regarding
41 changes in muscle coordination. Therefore, it is essential to explore the muscle synergy
42 patterns in individuals with APTA.

43 **Methods:** This study recorded sEMG data during stop-jump tasks in 8 APTA and 8
44 healthy amateur male basketball players in a simulated basketball game. Muscle
45 synergies were extracted using Non-Negative Matrix Factorization and K-Means
46 clustering.

47 **Results:** Three synergies were identified in both groups. In Synergy 1, tibialis anterior,
48 semitendinosus, and vastus lateralis weights primarily influenced the waveform. In
49 Synergy 2, biceps femoris, vastus lateralis and medial gastrocnemius weights primarily
50 influenced the waveform. In Synergy 3, peroneus longus, vastus medialis, and vastus
51 lateralis weights primarily influenced the waveform. Key findings include higher vastus
52 medialis weight in the APTA group during P1 and P2, and higher semitendinosus
53 weight in P3 and P4. Additionally, the gastrocnemius and biceps femoris showed
54 significant differences between groups across phases.

55 **Conclusions:** The APTA group exhibited different muscle synergy patterns under
56 specific phases and load accumulation conditions, particularly in the vastus medialis,
57 medial gastrocnemius, biceps femoris, and peroneus longus. The APTA group
58 demonstrated distinct synergy patterns, suggesting a compensatory mechanism to
59 reduce patellar tendon load, potentially increasing knee injury risk. This finding
60 provides new guidance for clinical assessment and intervention strategies for the
61 training and rehabilitation of APTA individuals.

62

63 **Keywords:** asymptomatic patellar tendon abnormalities; basketball exercise simulation;
64 motor control; K-means clustering; non-negative matrix factorization.

65

66 **1. Introduction**

67 Patellar tendinopathy (PT) is a common overuse injury of the knee, frequently occurring

68 in sports involving repetitive jumping and landing. A multidisciplinary sports club study
69 conducted over eight seasons found that the incidence of PT among professional
70 basketball players was 22.7%, with guards exhibiting the highest incidence due to the
71 frequent jumping involved in their position[36]. Given the high incidence of PT and its
72 severe impact on athletes' careers, understanding the injury mechanisms of patellar
73 tendinopathy and developing effective prevention strategies are particularly important.

74 The clinical diagnosis of PT is based on the patient's symptoms (such as patellar tendon
75 pain), while ultrasound imaging is considered the standard tool for diagnosing patellar
76 tendon abnormality (PTA). On ultrasound images, PTA typically appears as a
77 hypoechoic region. Previous studies have shown that PTA can be found even in
78 asymptomatic athletes, and this abnormality is often considered a precursor to PT[19].
79 Without timely rehabilitation treatment, PTA may gradually develop into PT, with an
80 occurrence probability of 22%-32%[35]. Although previous studies have compared
81 patellar tendinopathy patients with healthy individuals, the mechanisms by which PTA
82 evolves into patellar tendinopathy remain unclear [11, 21]. Therefore, this study
83 conducts a prospective study on individuals with asymptomatic patellar tendon
84 abnormality (APTA), to explore its relationship with the development of patellar
85 tendinopathy.

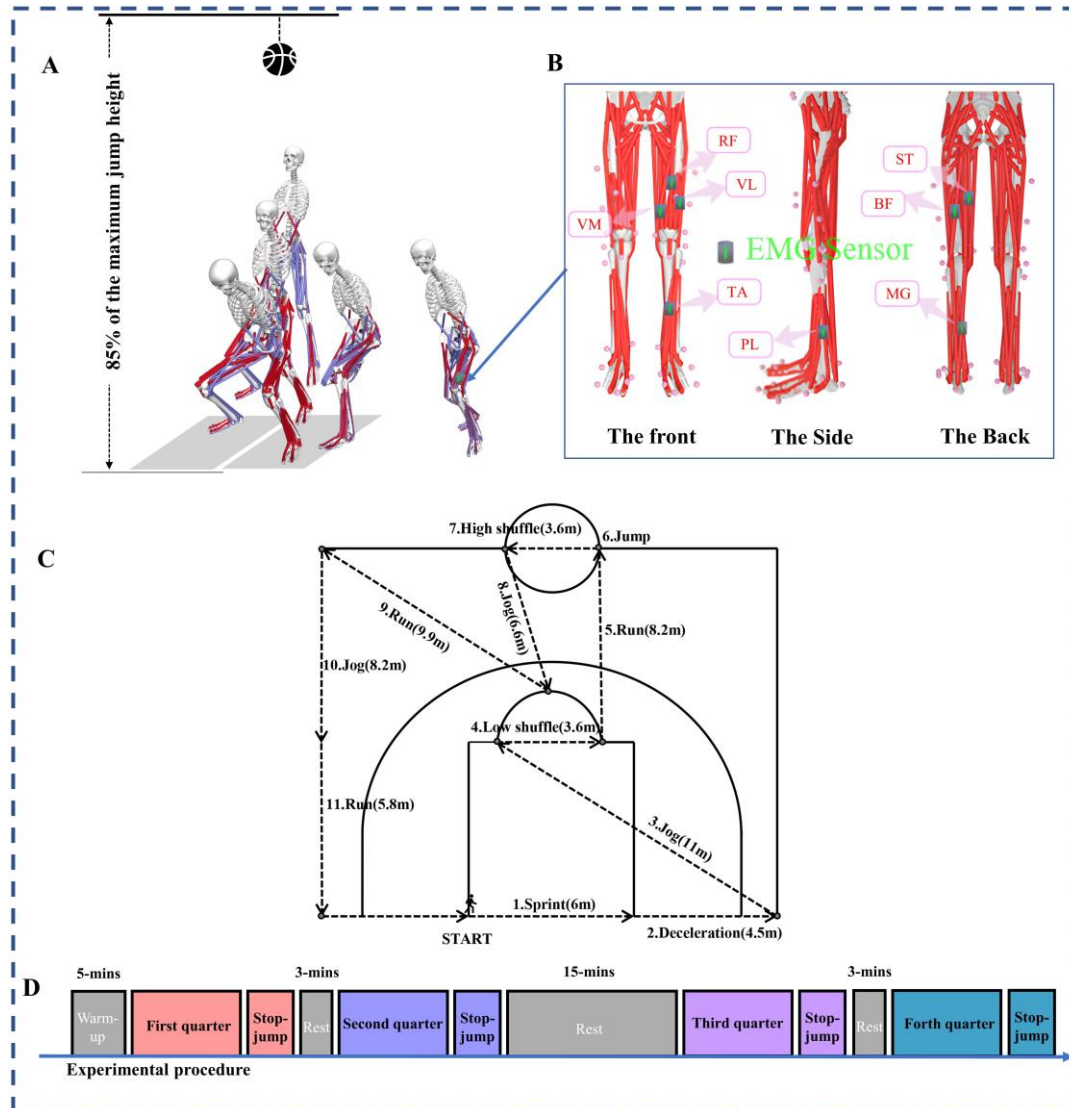
86 Studies have found that basketball players with PTA tend to reduce the load on the
87 patellar tendon during stop-jump maneuvers through compensatory mechanisms, such
88 as increased hip flexion[30]. Edwards et al.[10] discovered that during the horizontal
89 landing phase, PTA patients typically activate the semitendinosus (ST) and biceps
90 femoris (BF) first, while healthy individuals are more likely to first activate the tibialis
91 anterior (TA) and medial gastrocnemius (MG). These findings suggest that PTA patients
92 adjust their motor control strategies during stop-jump tasks to accommodate their
93 biomechanical changes or achieve better athletic performance[15]. **Although previous
94 studies have investigated the neuromuscular control strategies of athletes after knee
95 injuries, there is still a lack of systematic research on the specific changes in muscle
96 synergy patterns in individuals with asymptomatic patellar tendon abnormality (APTA)**

97 during high-load movement tasks[6]. At the same time, biomechanical characteristics
98 are actually the result of the nervous system interacting with the external environment
99 under task constraints and biomechanical limitations of the limbs[25]. Therefore,
100 analyzing only kinematic, kinetic, or individual muscle electrical activity
101 characteristics provides limited understanding of the specific impact of PTA on motor
102 control strategies[10]. Given the complex synergy among most muscles[22], accurately
103 identifying neuromuscular control strategies in specific tasks and gaining
104 comprehensive insights necessitates considering the synergistic interaction of multiple
105 muscles in an integrated manner. Therefore, it is important to study the specific changes
106 in muscle synergy patterns in the APTA population.

107 In recent years, scientists have employed a technique called Non-Negative Matrix
108 Factorization (NMF) to study the coordination of muscles during movement[26]. NMF
109 analysis helps identify the collaborative relationships between muscles and their
110 activation timing. In simple terms, muscle synergies function like a team, where
111 different muscles work together to perform specific actions, and the activation
112 coefficients indicate when this team is mobilized[26]. Because NMF is based on the
113 non-negativity of matrix factors, it offers greater interpretability of results, while also
114 being easy to implement and having low memory requirements[42]. Recently, NMF
115 has gradually expanded into the field of sports science and has shown potential in
116 enhancing athletic performance and preventing sports injuries[8, 20].

117 Based on the aforementioned research background, this study aims to explore the
118 impact of specialized loading on neuromuscular control strategies during stop-jump
119 tasks from the perspective of muscle synergies. It seeks to clarify the significance of
120 muscle synergies during different phases of the stop-jump task and analyze the synergy
121 differences between APTA and healthy individuals across different dimensions (time-
122 space). Understanding these differences is crucial for elucidating the pathogenesis of
123 patellar tendinopathy and developing prevention strategies. We hypothesize that there
124 will be no difference in the number of muscle synergies between the two groups, but
125 that the APTA group, compared to the healthy group, will exhibit different motor

126 modules by adjusting muscle activation weights to adapt to biomechanical changes
 127 induced by their condition.



128
 129 **Figure 1.** Experimental protocol. (A) The process of the stop-jump movement;
 130 (B) EMG marker location; (C) A schematic depiction of the Basketball Exercise
 131 Simulation Test (BEST); (D) The overall experimental process. BF: biceps femoris;
 132 MG: medial gastrocnemius; PL: peroneus longus; RF: rectus femoris; ST:
 133 semitendinosus; TA: tibialis anterior; VL: vastus lateralis; VM: vastus medialis;
 134 High = high-intensity; Low= low-intensity.

135

136 2. Materials and Methods

137 2.1 Subjects

138 A total of 8 asymptomatic PTA and 8 healthy amateur male basketball players were
 139 recruited for this study, with detailed participant information provided in Table 1.
 140 Inclusion criteria included: no history of professional basketball training; self-training
 141 1-2 times per week[27]. All participants were right-leg dominant and had no history of
 142 traumatic lower limb injury in the past 6 months[37]. Patellar tendon morphology was
 143 assessed by an experienced musculoskeletal ultrasound physician using a 13 MHz
 144 linear array portable ultrasound device (Siemens Antares, Siemens AG, Germany), with
 145 ultrasound abnormalities recorded. Ultrasound abnormalities were defined as
 146 hypoechoic areas ≥ 2 mm[4]. **Finally, 8 athletes showing patellar tendon abnormalities**
 147 **on ultrasound were assigned to the asymptomatic patellar tendon abnormality (APTA)**
 148 **group, and 8 matched healthy athletes were assigned to the control group.** All
 149 participants signed a written informed consent form before data collection. The study
 150 protocol was approved by the Scientific Research Ethics Committee of Ningbo
 151 University (Approval Number: RAGH20231120).

152 **Table 1.** Information of the eligible participants.

Variable	APTA (n = 8)	Healthy (n = 8)	p
	Mean (SD)	Mean (SD)	
Age (yrs)	23.0 (3.5)	22.8 (4.0)	0.693
Height (m)	1.80 (0.6)	1.82 (0.7)	0.602
Weight (kg)	75.0 (8.5)	77.1 (8.1)	0.557
BMI (kg/m ²)	23.9 (3.1)	23.5 (3.0)	0.654
Basketball experience (yrs)	5.5 (3.1)	5.1 (2.5)	0.434
Position of play	Point Guard	Point Guard	/

153 Note: SD: standard deviation; APTA: Asymptomatic Patellar Tendon Abnormality.

154 2.2 Procedures

155 2.2.1 Experiments

156 The Basketball Exercise Simulation Test (BEST) consists of four 10-minute phases,
 157 strictly following official game time. Each BEST cycle includes 30 seconds of
 158 intermittent specific exercises, incorporating activities such as sprinting, jumping,
 159 running, jogging, sliding, and recovery[34]. Figure 1C shows the various activities and
 160 distances involved in each BEST cycle. Each cycle is limited to 30 seconds, requiring

161 participants to perform continuously within each 10-minute interval (up to 20 cycles).
162 Typically, participants complete a cycle within 25 seconds, allowing at least 5 seconds
163 of rest to prepare for the next cycle. If participants fail to complete a cycle within the
164 allotted time, they must stop immediately and begin the next cycle. The overall
165 experimental procedure is shown in Figure 1D.

166 Before the experiment, participants underwent a 5-minute standardized dynamic warm-
167 up, including full-body dynamic and static stretching. In the main task of the
168 experiment, participants took a step forward from a self-selected distance, firmly
169 planting each foot on the ground, and then performed a vertical jump, attempting to
170 touch a ball on the ceiling with their dominant hand (Figure 1A). Prior to the experiment,
171 professional basketball players demonstrated and explained the tasks to ensure that all
172 participants were familiar with the procedure and to ensure consistency in data
173 collection. The criteria for successfully completing the stop-jump task were: (1) both
174 feet must fully contact the ground; (2) participants must touch the ball on the ceiling.
175 Participants were required to perform five stop-jumps, with the middle three trials used
176 for further analysis. During the experiment, all subjects wore their own sports shoes [15,
177 40].

178 2.2.2 Data Recording and Preprocessing

179 According to the SENIAM guidelines for sEMG sensor placement and anatomical
180 knowledge, the corresponding muscle locations were determined through a series of
181 specific movements. The optimal positions on the muscle bellies were selected by an
182 experienced researcher to ensure that the sensors were placed away from tendons or the
183 edges of muscles [17]. Before electrode placement, excess hair was removed using a
184 disposable razor, and the skin surface was carefully cleaned with 75% medical alcohol
185 to remove oil and debris. The skin was allowed to dry to minimize skin impedance
186 before attaching the electrodes. Using the EMGworks system (Delsys, Boston, USA),
187 eight sEMG sensors were placed on the muscle bellies at predetermined locations:
188 biceps femoris (BF) (50% of the distance between the ischial tuberosity and the lateral
189 epicondyle of the tibia), medial gastrocnemius (MG) (at the most prominent bulge of

190 the muscle), peroneus longus (PL) (at 25% of the line between the head of the fibula
191 and the lateral malleolus), rectus femoris (RF) (50% of the line between the anterior
192 superior iliac spine and the upper part of the patella), semitendinosus (ST) (50% of the
193 distance between the ischial tuberosity and the medial epicondyle of the tibia), tibialis
194 anterior (TA) (on the upper third of the line between the lateral condyle of the tibia and
195 the medial malleolus), vastus lateralis (VL) (on the upper two-thirds of the line from
196 the anterior superior iliac spine to the lateral side of the patella), and vastus medialis
197 (VM) (at 80% of the line between the anterior superior iliac spine and the medial joint
198 space of the knee). The sampling frequency was set to 1000Hz, and all sEMG electrodes
199 were aligned parallel to the direction of the muscle fibers, with an inter-electrode
200 distance of 10mm. Only data from the left limb were analyzed in this study, as the non-
201 dominant leg is more frequently used for jumping and landing during layups in
202 basketball[2, 19].

203 The preprocessing of sEMG signals was implemented using Matlab R2023b
204 programming. First, the baseline of the raw sEMG data was zeroed. Then, a 4th-order
205 Butterworth band-pass filter with a high-pass cutoff frequency of 30 Hz was applied to
206 the raw sEMG signal to remove motion artifacts. Afterward, the signal was
207 downsampled and full-wave rectified, followed by applying a 4th-order Butterworth
208 low-pass filter with a cutoff frequency of 20 Hz to the rectified signal to extract the
209 linear envelope[32]. Finally, all sEMG envelopes were interpolated to match the
210 sampling point length of the same movement cycle and normalized to the maximum
211 amplitude of the envelope during the stop-jump action [28].

212 2.2.3 Non-Negative matrix factorization extracts muscle synergies

213 This study employed a Non-Negative Matrix Factorization (NMF) framework to extract
214 muscle synergy components from sEMG data through linear decomposition based on
215 unsupervised machine learning, with computations performed on the Rv4.4.1 platform.
216 NMF decomposed the preprocessed sEMG signal matrix $V_{m \times n}$ into two non-negative
217 matrices, as shown in Equation (1).

$$V_{m \times n} = [EMG_1 \ EMG_2 \dots \ EMG_m]^T \approx (WH)_{m \times n} = \sum_{i=1}^p W_{m \times p} H_{p \times w} + e = V'_{m \times n} \quad (1)$$

218 In this equation, V represents the original sEMG matrix, where M denotes the number
 219 of sEMG channels, and N denotes the number of samples. P is the number of muscle
 220 synergies obtained through NMF, where $M \geq P \geq 1$. $W_{m \times p}$ represents the muscle
 221 synergy vectors, and $H_{p \times w}$ represents the time activation coefficients. The
 222 reconstructed matrix $V'_{m \times n}$ is obtained by multiplying the W and H matrices and then
 223 adding the residual term e.

224 During the extraction of the basis and coefficient matrices using the Gaussian NMF
 225 Multiplicative Update Rules, the iteration stops when the R^2 change is less than 0.01%
 226 for 20 consecutive iterations, reaching the convergence threshold[32]. The quality of
 227 the NMF reconstruction is evaluated by the variance accounted for (VAF) to determine
 228 the optimal number of synergies. The steps for calculating VAF are as follows:

$$VAF = \left(1 - \frac{RSS}{TSS}\right) \times 100\% = \left(1 - \frac{\sum(V - V')^2}{\sum(V - \bar{V})^2}\right) \times 100\% \quad (2)$$

229 Where: RSS refers to the residual sum of squares, and TSS refers to the total sum of
 230 squares. V represents the original muscle activation matrix. V' represents the NMF-
 231 reconstructed data matrix. \bar{V} represents the mean of the original matrix V. To
 232 determine the optimal number of synergy components, this study calculated the VAF
 233 for the 1st to 6th order NMF decomposition results, and this was used to evaluate the
 234 optimal order, as shown in Table 2.

235 VAF > 90% is commonly used in the literature to identify the optimal number of
 236 synergies[31]. This criterion is considered to sufficiently represent the data, although
 237 its application remains debated[1]. For ease of comparison between groups, we selected
 238 the same number of muscle synergies as the rounded average of the synergies across all
 239 participants for further analysis[43]. The K-Means algorithm was used to cluster the
 240 muscle synergies of the APTA and Healthy groups separately, obtaining the overall
 241 synergy characteristics of athletes in different groups.

242 2.2.4 Statistical analysis

243 Muscle synergy data were processed using SPSS 23 statistical software, with results
 244 presented as means and standard deviations. To compare the differences in weight
 245 contributions of different muscles in each synergy, we conducted a two-way repeated
 246 measures ANOVA for each synergy. The two factors analyzed were group (APTA group
 247 and Healthy group) and load phase (P1, P2, P3, P4). When significant main effects or
 248 interaction effects were found, post hoc Bonferroni tests were used to further reveal
 249 specific differences. For violations of the sphericity assumption, we made adjustments
 250 using the Greenhouse-Geisser correction. Effect sizes were calculated using partial eta
 251 squared (η^2) to assess the magnitude of differences: <0.06 for small effects, $0.07-0.14$
 252 for medium effects, and >0.14 for large effects.

253 **3 Results**

254 *3.1. Choosing the Optimal Number of Synergies under NMF*

255 Muscle synergies can reflect the neuromuscular control strategies employed by athletes
 256 when performing movements[33]. Figure 2 shows the VAF of muscle synergies in the
 257 APTA and Healthy groups across the four phases. The interaction between groups and
 258 load accumulation on VAF was not statistically significant, $F(3, 21) = 0.661$, $p = 0.541$,
 259 $\eta^2 = 0.02$. Table 2 shows that the number of muscle synergies in the APTA and Healthy
 260 groups at each phase were 3.02, 3.10, 3.11, and 3.10, and 3.20, 3.10, 3.05, and 3.19,
 261 respectively. To further compare the muscle synergy structures between groups, we
 262 rounded the number of synergies to 3. The results showed that when 3 muscle synergies
 263 were extracted, the VAFs for the APTA and Healthy groups at the four phases were
 264 90.23%, 92.15%, 95.01%, and 95.21%, and 93.11%, 93.55%, 91.13%, and 92.56%,
 265 respectively. The average VAF within all groups exceeded 90%. However, when the
 266 number of synergies increased to 4, the average VAF improvement was less than 2%,
 267 so the number of synergies was ultimately set at 3 for further analysis.

268 **Table 2.** The relationship between the number of synergies and VAF: The number of
 269 synergies is determined when VAF first exceeds 0.9.

Group	P1 Mean (SD)	P2 Mean (SD)	P3 Mean (SD)	P4 Mean (SD)	P
-------	-----------------	-----------------	-----------------	-----------------	---

Num of Syn	APTA	3.02(0.02)	3.10(0.05)	3.11(0.05)	3.10(0.1)	0.522
	Healthy	3.20(0.07)	3.10(0.07)	3.05(0.01)	3.19(0.12)	0.310
	p	0.179	0.677	0.535	0.257	
VAF (%)						
2 Syn	APTA	78.23(5.12)	82.43(4.86)	85.66(5.19)	90.33(5.55)	0.097
	Healthy	81.46(4.71)	81.67(4.19)	80.57(5.59)	86.31(4.35)	0.355
	p	0.132	0.443	0.175	0.223	
3 Syn	APTA	90.23(3.15)	92.15(4.01)	95.01(2.23)	95.21(2.21)	0.294
	Healthy	93.11(2.31)	93.55(2.32)	91.13(4.33)	92.56(3.44)	0.501
	p	0.367	0.621	0.211	0.387	
4 Syn	APTA	93.00(2.01)	95.04(2.09)	94.09(1.44)	95.21(1.12)	0.621
	Healthy	94.01(2.00)	95.11(1.86)	94.22(1.03)	95.00(1.02)	0.533
	p	0.667	0.659	0.721	0.763	

Note: P1: phase 1; P2: phase 2; P3: phase 3; P4: phase 4; SD: standard deviation; Num of Syn: the number of muscle synergies; VAF: variability accounted for; APTA: Asymptomatic Patellar Tendon Abnormality.

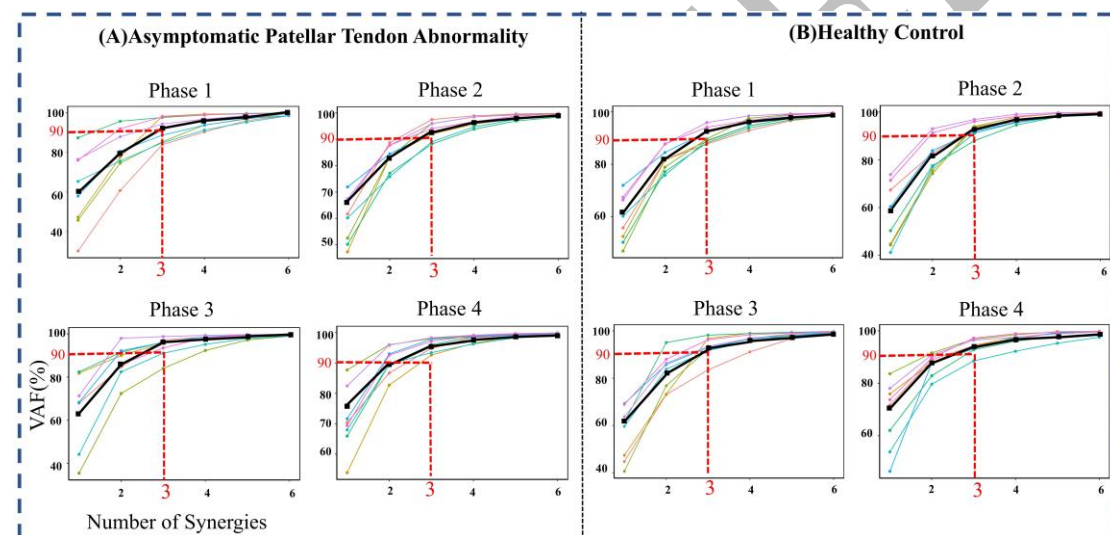
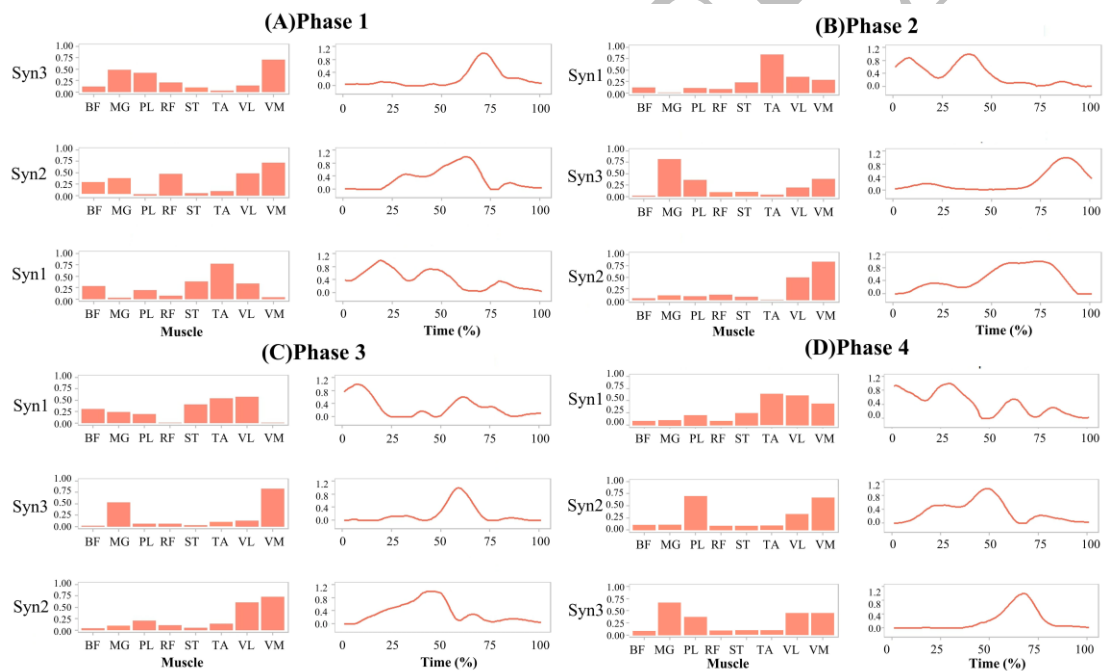


Figure 2. Individual (thin line) and mean participant (thick lines) percentages of the variability accounted for (VAF). (A) and (B) panels show the VAFs of the APTA and the healthy group, respectively. The horizontal dashed lines indicate the thresholds used to determine the number of extracted lower limb muscle synergies.

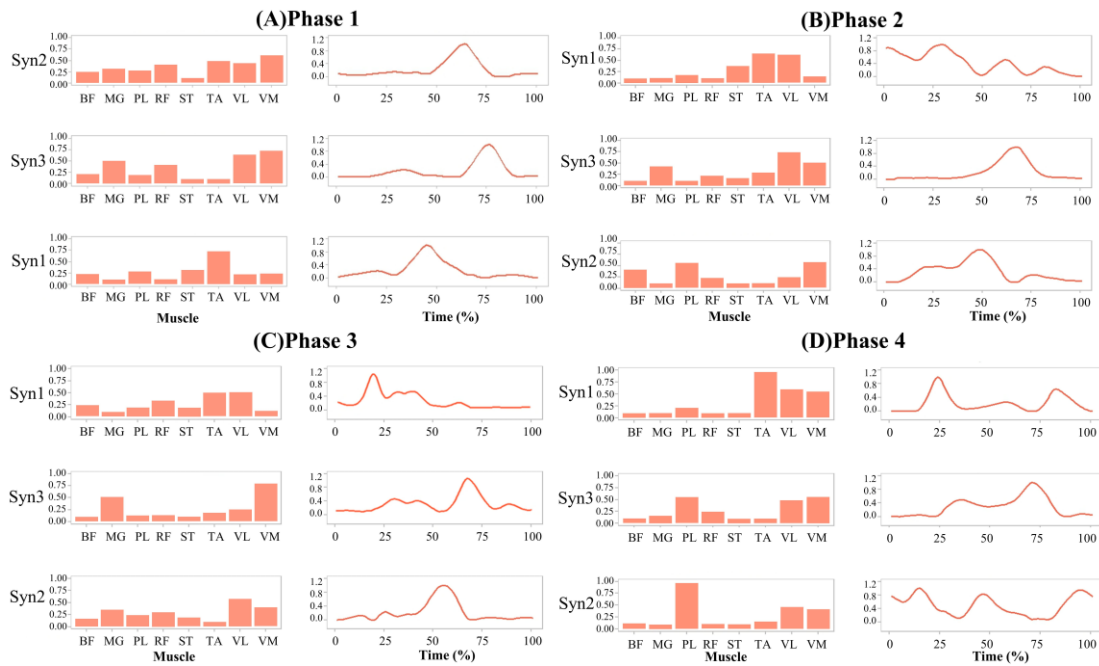
3.2. Features of Muscle Synergy Extraction

Figure 3 and 4 illustrate the muscle weights and temporal activation patterns during the stop-jump process for the APTA and Healthy groups across the four phases, respectively. Figure 5 provides a heatmap of the muscle weights in the lower limbs during the stop-jump across the four phases for the APTA and Healthy groups. Based on the temporal structure, the classification of muscle synergies corresponds to specific movement

283 phases during the stop-jump process, with each cycle consisting of three distinct phases:
 284 initial ground contact, braking, and vertical jump phases. Based on the timing of peak
 285 occurrence, the waveform of Synergy1 is associated with the initial ground contact
 286 phase of the stop-jump, with the peak appearing at the start of the action (0 - 30%) and
 287 then declining. The waveform of Synergy1 is mainly influenced by the weights of TA,
 288 ST, and VL. The main peak of Synergy2 appears in the braking phase (30% - 60%),
 289 with activation increasing during this phase and then decreasing. The waveform of
 290 Synergy2 is mainly determined by the weights of BF, ST, VL, VM, and MG. The
 291 waveform of Synergy3 appears during the vertical jump phase (60% - 100%), and is
 292 mainly determined by the weights of VL, VM, RF, PL, and MG.



293
 294 **Figure 3.** The muscle synergy extraction for the APTA group. (A), (B), (C), and (D)
 295 represent the muscle synergies for P1, P2, P3, and P4, respectively, extracted from 8
 296 leg muscles and used for functional classification during the stop-jump movement.
 297 Left: muscle weights; Right: activation patterns; Syn: Synergy.



298

299 **Figure 4.** The muscle synergy extraction for the Healthy group. (A), (B), (C), and (D)
 300 represent the muscle synergies for P1, P2, P3, and P4, respectively, extracted from 8
 301 leg muscles and used for functional classification during the stop-jump movement. Left:
 302 muscle weights; Right: activation patterns; Syn: Synergy.

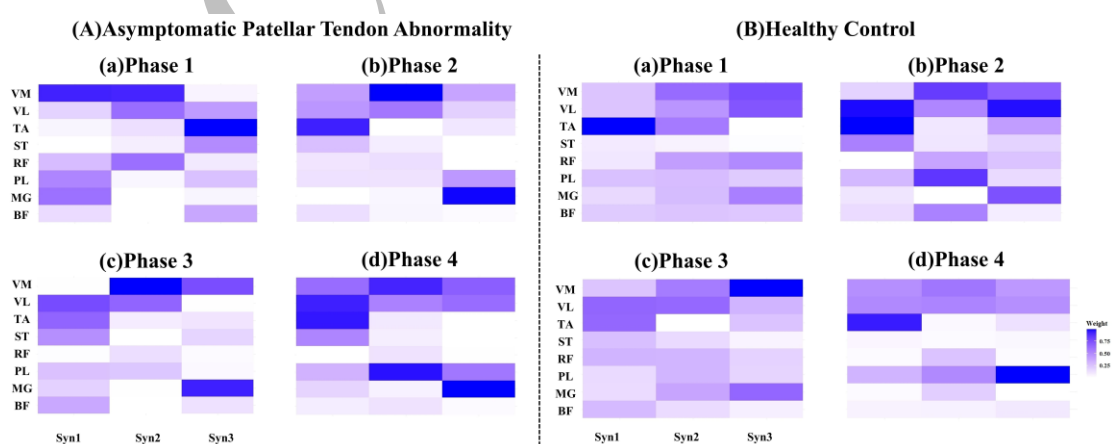
303 3.3. APTA and Healthy group differences in each synergy across four loading phases

304 Figure 6 provides a detailed overview of the muscle weight comparison between the
 305 APTA and Healthy VMs across the four phases in the three synergies. In Synergy 1,
 306 the interaction between groups and load accumulation for VM has statistical
 307 significance, $F(3, 21) = 2.669$, $p = 0.041$, $\eta^2 = 0.16$. The interaction between groups and
 308 load accumulation for ST is statistically significant, $F(3, 21) = 3.022$, $p = 0.038$, $\eta^2 =$
 309 0.19 . Specifically, the VM weight in the APTA group was significantly higher than that
 310 in the Healthy group during the P1 and P2, with differences of 0.45 and 0.25,
 311 respectively ($p < 0.05$). Meanwhile, in the P3 and P4, the ST weight in the APTA group
 312 was significantly higher than that in the Healthy group, with differences of 0.18 and
 313 0.30, respectively ($p < 0.05$).

314 In Synergy 2, the interaction between groups and load accumulation for MG is
 315 statistically significant, $F(3, 21) = 3.135$, $p = 0.035$, $\eta^2 = 0.19$. The interaction between
 316 groups and load accumulation for BF is statistically significant, $F(3, 21) = 5.266$, $p =$

317 0.021, $\eta^2 = 0.26$. Specifically, the MG muscle weight in the Healthy group was
 318 significantly higher than in the APTA group at all phases, with differences of 0.18, 0.17,
 319 0.14, and 0.12, respectively ($p < 0.05$). Additionally, the BF weight in the Healthy group
 320 was significantly higher than in the APTA group during the P1 and P2 phases, with
 321 differences of 0.18 and 0.25, respectively ($p < 0.05$).

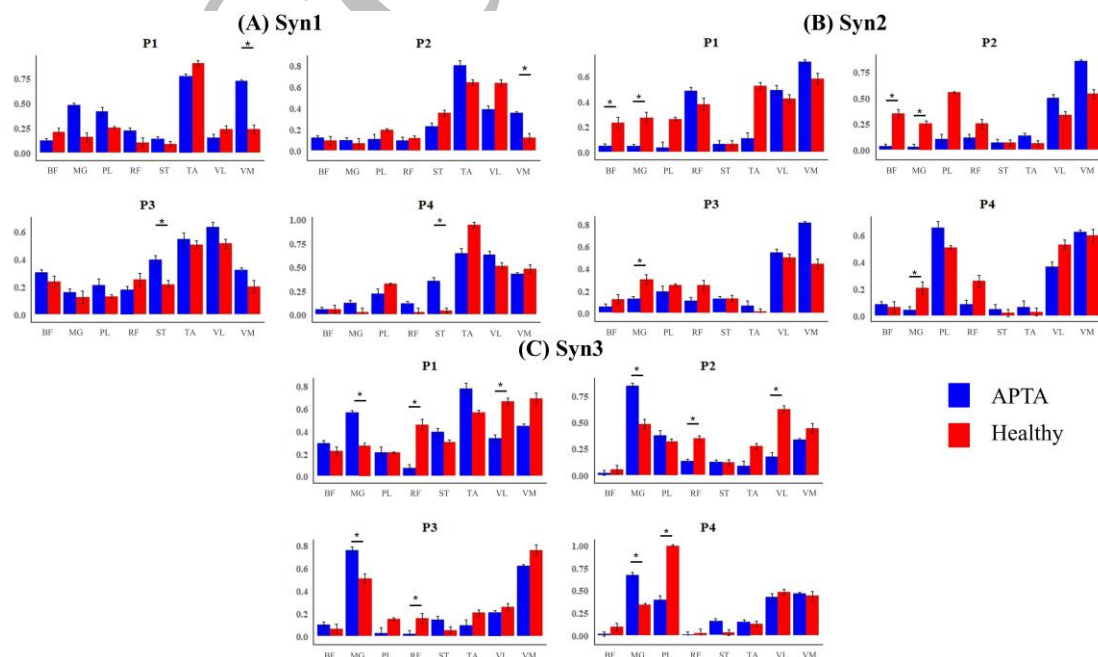
322 In Synergy 3, the interaction between groups and load accumulation for MG is
 323 statistically significant, $F(3, 21) = 6.031$, $p = 0.005$, $\eta^2 = 0.43$. The interaction between
 324 groups and load accumulation for RF is statistically significant, $F(3, 21) = 5.771$, $p =$
 325 0.009 , $\eta^2 = 0.36$. The interaction between groups and load accumulation for VL is
 326 statistically significant, $F(3, 21) = 5.012$, $p = 0.017$, $\eta^2 = 0.25$. Specifically, the MG
 327 weight in the APTA group was significantly higher than in the Healthy group at all four
 328 phases, with differences of 0.33, 0.31, 0.28, and 0.43 ($p < 0.05$), while the Healthy
 329 group showed significant advantages in RF and VL at multiple phases. Specifically, the
 330 RF weight in the Healthy group was significantly higher than in the APTA group during
 331 the P1, P2, and P3 phases, with differences of 0.35, 0.21, and 0.12, respectively ($p <$
 332 0.05). The VL weight in the Healthy group was also significantly higher than in the
 333 APTA group during the P1 and P2 phases, with differences of 0.35 and 0.47,
 334 respectively ($p < 0.05$).



335
 336 **Figure 5.** Heatmap of muscle weights during the 4 phases of the stop-jump for the
 337 APTA and the healthy group. Syn: Synergy.

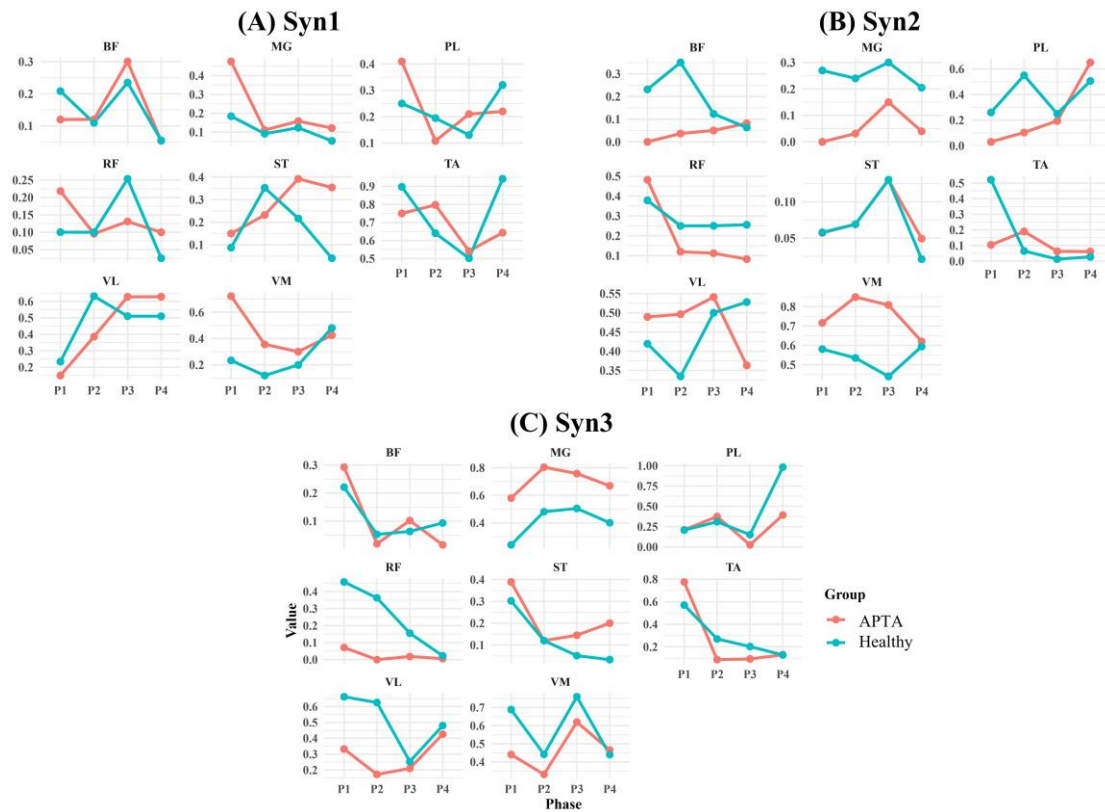
338 *3.4. The trend of lower limb muscle weight in the APTA and the Healthy group across*

340 Figure 7 shows the trends in lower limb muscle weights across the four phases in the
 341 APTA and Healthy groups under the three synergies. In Synergy 1, the relative weight
 342 of the ST in the APTA group was low in P1 but significantly increased in phases P2 and
 343 P3 ($p < 0.05$). The TA had a higher weight in P1 but significantly decreased in phases
 344 P2 and P3 ($p < 0.05$). The VL exhibited low activity in P1, which significantly increased
 345 in P2 and P3 ($p < 0.05$). The muscle activity in the Healthy group was relatively stable
 346 across all four phases. In Synergy 2, the VM and MG in the APTA group showed low
 347 activity in P1 but significantly increased in P2 and P3 ($p < 0.05$). The BF in the APTA
 348 group had higher activity in P1, then gradually decreased ($p < 0.05$). The PL exhibited
 349 higher activity in P1, followed by a significant decrease in P2 and P3 ($p < 0.05$). The
 350 BF in the Healthy group had low activity in P1 and P2, but significantly increased in
 351 P3 and P4 ($p < 0.05$). The activity of other muscles remained relatively stable. In
 352 Synergy 3, the MG, RF, and ST in the APTA group had low activity in P1 but
 353 significantly increased in P2 and P3 ($p < 0.05$), while the PL had high activity in P1 but
 354 significantly decreased in P2 and P3 ($p < 0.05$). The muscle activity in the Healthy
 355 group remained stable across all four phases.



356

357 **Figure 6.** Diagram of the differences in muscle weights across three synergies during



359

360 **Figure 7.** The activity trend chart of the APTA and the Healthy group in three synergies
 361 across four phases. Syn: Synergy.

362 4 Discussion

363 This study aims to investigate the muscle synergy patterns in the APTA individuals
 364 during the stop-jump task. To our knowledge, this study is the first to quantitatively
 365 detail the modular organization strategy of neuromotor responses in APTA individuals
 366 during stop-jump. This study reveals the following key findings: (1) APTA individuals
 367 exhibit higher ST activity during the landing phase of stop-jump, emphasizing its
 368 critical role in the central nervous system's modular control strategy. (2) During the
 369 braking phase, APTA individuals exhibit deficiencies in the coordination of multi-
 370 muscle control, particularly in the altered spatial and temporal patterns of muscle
 371 synergies involving the BF and MG. (3) During the vertical jump phase, APTA
 372 individuals display an abnormal muscle synergy pattern with higher MG activity
 373 contribution and lower VM and VL contributions, which may be an adaptive response.

374 The results support our hypothesis that there is no significant difference in the number
375 of muscle synergies between the two groups; APTA individuals may adapt to
376 biomechanical changes induced by their condition by adjusting the activity weights of
377 different muscles within each motor module.

378 In our analysis, we included 8 lower limb muscles because we focused on the synergies
379 between muscles during the stop-jump. We analyzed the four phases of load
380 accumulation in both APTA and Healthy individuals to effectively reveal motor
381 control deficits in the APTA individuals [2, 11, 14]. However, our findings indicate that
382 there is no significant difference in the VAF of the three extracted synergies between
383 the groups. Overall, the muscle synergies and their temporal patterns were strikingly
384 similar between the two groups. This aligns with previous research on APTA
385 individuals during the stop-jump task, indicating that despite variations in motor
386 performance, APTA individuals mobilize similar muscle synergies through
387 compensatory mechanisms to effectively execute the stop-jump task[38]. **This also
388 supports the existing view that neuromuscular adaptations do not necessarily alter the
389 overall structure of motor modules but rather modify the activation patterns within
390 existing modules[7]. This provides a new perspective, revealing that despite underlying
391 pathologies, muscle synergies remain relatively stable. This finding is of significant
392 importance for rehabilitation strategies aimed at maintaining neuromuscular function.**
393 Even in the presence of underlying tendon abnormalities, the neuromuscular system
394 may maintain a similar motor pattern through adaptive adjustments, which could
395 explain the lack of significant differences in synergy patterns.

396 At a functional level, the muscle synergies obtained in this study correspond to the
397 previously described biomechanical characteristics of stop-jump. A complete stop-jump
398 cycle includes the initial ground contact phase, the braking phase, and the vertical take-
399 off phase. In the initial ground contact phase (0-30%), the primary muscles involved
400 are the TA, ST, and VL, with TA activity initiating at ground contact (as indicated in
401 Figure 3A's syn1), likely to stabilize the ankle during early dorsiflexion[13]. With load
402 accumulation, the TA's weight contribution diminishes in P3 (Figure 7A), possibly

403 causing ankle instability and reducing the ankle's ability to absorb ground impact due
404 to decreased TA eccentric contraction, thus increasing knee stress and the risk of knee
405 injury[9]. Therefore, APTA individuals s need to strengthen the power and endurance
406 of ankle flexors and enhance eccentric contraction muscles like ST to better control
407 knee flexion. In the P1 and P2, there is a difference in the VM weight contribution to
408 Syn1 between the APTA and Healthy groups (Figure 6A). During initial ground contact,
409 the VM weight contribution in the APTA group is higher than in the Healthy group,
410 indicating a compensatory mechanism, possibly through increased VM activation to
411 stabilize the knee and prevent excessive flexion or instability. The eccentric contraction
412 of VM helps absorb impact and slow down knee flexion, thereby reducing stress on the
413 patellar tendon[41]. With load accumulation, ST's weight contribution peaks in P3
414 (Figure 7A). As a knee flexor, ST is closely related to knee flexion during the stop-jump.
415 During the landing phase, the eccentric contraction of ST helps absorb ground reaction
416 forces, reducing knee impact[29]. This study uses NMF to further emphasize the
417 importance of TA, ST, and VM in neuromotor control among APTA individuals s and
418 reveals a clinical phenomenon: APTA individuals s adapt to increased loads by
419 enhancing the strength and stability of ankle muscles and strengthening knee flexors to
420 absorb more impact.

421 Dorsiflexion during the braking phase (30%-60%) is accompanied by subsequent
422 knee flexion. In the recorded muscle activity of this study, BF, ST, VL, VM, and MG
423 are responsible for knee flexion, explaining the additional activity of BF and MG in
424 synergy1. We observed deficits in multi-muscle coordination control during the braking
425 phase in the APTA individuals, as evidenced by changes in the spatial and temporal
426 patterns of BF and MG muscle synergies. Figure 6B shows that the MG activation
427 weight in the APTA group was significantly lower than that in the Healthy group across
428 all four phases, with BF activation also notably lower in P1, P2, and P4. This supports
429 earlier findings that the APTA group tends to rely on other muscles by adjusting motor
430 module functions, resulting in reduced BF and MG activation[39]. Previous studies
431 have found that pain-avoidance strategies and long-term joint abnormalities affect

432 muscle activation patterns[18]. Although APTA individuals do not exhibit obvious pain
433 symptoms, chronic patellar tendon abnormalities may subconsciously lead them to
434 adopt pain-avoidance strategies to reduce pressure on the patellar tendon. This strategy
435 might reduce their reliance on muscles associated with the patellar tendon region (e.g.,
436 BF and MG) during the landing cushioning phase, thereby lessening the tensile and
437 shear forces on the patellar tendon. **Individuals with musculoskeletal abnormalities**
438 **adapt neuromuscular control by redistributing muscle activity to reduce the load on the**
439 **affected tendons[23]. This finding further confirms that the CNS adjusts motor control**
440 **strategies to protect vulnerable areas, thereby reducing the risk of injury aggravation.**
441 As load accumulates, the activation weight of VM and MG increases, while the
442 activation weight of BF and PL decreases, as shown in Figure 7B. Thus, APTA
443 individuals might enhance knee control by increasing VM and MG activation to prevent
444 excessive knee flexion, thereby reducing patellar tendon load. Previous studies have
445 shown that people with patellar tendinopathy use protective strategies under fatigue to
446 avoid additional stress on the patellar tendon, including proximal compensation and
447 stiff lower limb landing[40], which aligns with the conclusions of this study. PL helps
448 counter the inversion stress generated during landing in the stop-jump, aiding in
449 resisting varus or valgus torques at the knee and further ensuring joint stability. This
450 phenomenon is observed not only in Synergy2 but also in Synergy3. Consequently,
451 APTA individuals face an increased risk of injury during load accumulation. Therefore,
452 APTA individuals are advised to strengthen VM and MG through power training, while
453 also enhancing BF and PL endurance [3].

454 The vertical take-off phase (60%-100%) typically involves the activation of the hip
455 extensors, knee extensors, and ankle flexors[24]. In the initial phase of the ascent, VM
456 and VL contribute most of the concentric movement, while the contribution of the
457 gastrocnemius gradually increases in the later phase[12]. **However, we noticed that in**
458 **the early ascent phase, the APTA group displayed an abnormal muscle synergy pattern,**
459 **with higher MG activity and relatively lower contributions from VM and VL (Figure**
460 **6C). In actual competition, pressure, tension, and the game outcome can all affect**

461 neuromuscular control. However, the simulated game environment lacks these
462 psychological factors, which may lead to insufficient muscle activation in athletes.
463 Previous studies have shown that insufficient quadriceps activation can lead to
464 inadequate knee extension[16]. We also found that the effect size of the interaction
465 between group and load accumulation for MG reached 0.43, indicating that as the load
466 changes, APTA individuals may adapt their knee joint load by adjusting MG activation
467 to reduce the burden on the knee joint, thereby lowering the risk of injury. Consequently,
468 APTA individuals may compensate for insufficient knee extension by increasing
469 gastrocnemius activation, providing more force during the initial phase of the jump.
470 The recruitment sequence and relative contribution from hip extensors to knee
471 extensors and finally to ankle flexors can also be observed in similar movements, such
472 as reverse jumping or transitioning from sitting to standing. This might indicate that
473 stable motor patterns naturally develop after mastering complex lower limb movements.
474 When discussing muscle synergy, the number of muscles chosen and the number of
475 synergies selected significantly influence the results. In this study, we focused only on
476 the 8 lower limb muscles, as the research emphasized the synergy between these
477 muscles during the stop-jump process. However, future research should further explore
478 the contribution of upper limb muscles (e.g., latissimus dorsi) and trunk muscles (e.g.,
479 erector spinae, rectus abdominis, and external oblique) to assess the relationship
480 between upper and lower limb muscle synergy in complex movements. Moreover, this
481 study was carried out in a laboratory environment, with strictly controlled conditions,
482 but it could not entirely simulate the complexities of a real basketball game. Therefore,
483 future research should consider being conducted on an actual basketball court to
484 observe athletes' muscle synergies during real game situations. Another limitation of
485 this study is its short duration, making it difficult to determine whether motor module
486 control causes injuries or if injuries lead to changes in motor module control. Future
487 research should involve long-term prospective studies to further investigate this causal
488 relationship. Additionally, the use of dimensionality reduction techniques is also a topic
489 of debate. Some researchers argue that specific muscle synergies reflect motor

490 commands specifically adjusted by the central nervous system for particular tasks,
491 while others suggest that these synergies might simply be artifacts of the decomposition
492 algorithm used[5]. Regardless of the viewpoint, further research is needed to explore
493 the underlying mechanisms of these muscle synergies. Future research should broaden
494 its scope to cover more motor tasks, providing a more comprehensive understanding of
495 motor module control in the APTA individuals.

496 **5 Conclusions**

497 The main purpose of this study was to investigate the muscle synergy patterns of the
498 APTA individuals during the stop-jump. The results showed that although there were
499 no significant differences in the number of muscle synergies and the VAF of the
500 extracted synergy patterns between the APTA and healthy groups, the APTA group
501 exhibited significantly abnormal muscle synergy patterns in specific phases and under
502 load accumulation conditions. These abnormalities mainly occurred in the ST, MG, BF,
503 and PL, suggesting that APTA individuals might use compensatory mechanisms to
504 avoid excessive load on the patellar tendon. However, this compensatory strategy may
505 increase the risk of injury to the knee joints. Therefore, training for APTA individuals
506 should focus on strengthening the ST and MG muscles and improving the endurance of
507 the BF and PL muscles to enhance joint stability and prevent patellar tendinopathy.

508

509 **Funding**

510 This study was sponsored by Zhejiang Province Key R&D program of “Pioneer” and
511 “Leader” (2023C03197), Zhejiang Province Science Fund for Distinguished Young
512 Scholars (Grant number: LR22A020002), Ningbo Key Research and Development
513 Program (Grant number: 2022Z196), Zhejiang Rehabilitation Medical Association
514 Scientific Research Special Fund (ZKKY2023001), Research Academy of Medicine
515 Combining Sports, Ningbo (No.2023001), the Project of Ningbo Leading Medical
516 &Health Discipline (No.2022-F15, No.2022-F22), Ningbo Natural Science Foundation
517 (Grant number: 2022J065) and K. C. Wong Magna Fund in Ningbo University.

518

519 **Reference**

- 520 [1] Barradas VR, Kutch JJ, Kawase T, Koike Y, Schweighofer N. When 90% of the
521 variance is not enough: residual EMG from muscle synergy extraction influences
522 task performance. *J Neurophysiol.* 2020;123(6):2180-90.
- 523 [2] Benítez-Martínez JC, Valera-Garrido F, Martínez-Ramírez P, Ríos-Díaz J, Del
524 Baño-Aledo ME, Medina-Mirapeix F. Lower Limb Dominance, Morphology, and
525 Sonographic Abnormalities of the Patellar Tendon in Elite Basketball Players: A
526 Cross-Sectional Study. *J Athl Train.* 2019;54(12):1280-6.
- 527 [3] Challoumas D, Pedret C, Biddle M, Ng NYB, Kirwan P, Cooper B, et al.
528 Management of patellar tendinopathy: a systematic review and network meta-
529 analysis of randomised studies. *BMJ Open Sport Exerc Med.* 2021;7(4):e001110.
- 530 [4] Cook JL, Khan KM, Kiss ZS, Coleman BD, Griffiths L. Asymptomatic
531 hypoechoic regions on patellar tendon ultrasound: A 4-year clinical and ultrasound
532 followup of 46 tendons. *Scand J Med Sci Sports.* 2001;11(6):321-7.
- 533 [5] Coscia M, Cheung VC, Tropea P, Koenig A, Monaco V, Bennis C, et al. The effect
534 of arm weight support on upper limb muscle synergies during reaching movements.
535 *J Neuroeng Rehabil.* 2014;11:22.
- 536 [6] d'Avella A. Modularity for Motor Control and Motor Learning. *Adv Exp Med Biol.*
537 2016;957:3-19.
- 538 [7] d'Avella A, Giese M, Ivanenko YP, Schack T, Flash T. Editorial: Modularity in
539 motor control: from muscle synergies to cognitive action representation. *Front*
540 *Comput Neurosci.* 2015;9:126.
- 541 [8] Dal Pupo J, Detanico D, Ache-Dias J, Santos SG. The fatigue effect of a simulated
542 futsal match protocol on sprint performance and kinematics of the lower limbs. *J*
543 *Sports Sci.* 2017;35(1):81-8.
- 544 [9] Dury J, Michel F, Ravier G. Fatigue of hip abductor muscles implies
545 neuromuscular and kinematic adaptations of the ankle during dynamic balance.
546 *Scand J Med Sci Sports.* 2022;32(9):1324-34.
- 547 [10] Edwards S, Steele JR, McGhee DE, Beattie S, Purdam C, Cook JL. Landing
548 strategies of athletes with an asymptomatic patellar tendon abnormality. *Med Sci*

-
- 549 Sports Exerc. 2010;42(11):2072-80.
- 550 [11] Edwards S, Steele JR, McGhee DE, Purdam CR, Cook JL. Asymptomatic players
551 with a patellar tendon abnormality do not adapt their landing mechanics when
552 fatigued. *J Sports Sci.* 2017;35(8):769-76.
- 553 [12] Escamilla RF. Knee biomechanics of the dynamic squat exercise. *Med Sci Sports
554 Exerc.* 2001;33(1):127-41.
- 555 [13] Fsm A, Fs O, Chbf J, Bms A, Vc D, editors. Analysis of electromyographic
556 patterns during standard and declined squats Análise do padrão eletromiográfico
557 durante os agachamentos padrão e declinado2009.
- 558 [14] Harris M, Schultz A, Drew MK, Rio E, Adams S, Edwards S. Thirty-seven jump-
559 landing biomechanical variables are associated with asymptomatic patellar tendon
560 abnormality and patellar tendinopathy: A systematic review. *Phys Ther Sport.*
561 2020;45:38-55.
- 562 [15] Harris M, Schultz A, Drew MK, Rio E, Charlton P, Edwards S. Jump-landing
563 mechanics in patellar tendinopathy in elite youth basketballers. *Scand J Med Sci
564 Sports.* 2020;30(3):540-8.
- 565 [16] Hart JM, Pietrosimone B, Hertel J, Ingersoll CD. Quadriceps activation following
566 knee injuries: a systematic review. *J Athl Train.* 2010;45(1):87-97.
- 567 [17] Hermens HJ, Freriks B, Disselhorst-Klug C, Rau G. Development of
568 recommendations for SEMG sensors and sensor placement procedures. *J
569 Electromyogr Kinesiol.* 2000;10(5):361-74.
- 570 [18] Hodges PW, Tucker K. Moving differently in pain: a new theory to explain the
571 adaptation to pain. *Pain.* 2011;152(3 Suppl):S90-s8.
- 572 [19] Hutchison MK, Houck J, Cuddeford T, Dorociak R, Brumitt J. Prevalence of
573 Patellar Tendinopathy and Patellar Tendon Abnormality in Male Collegiate
574 Basketball Players: A Cross-Sectional Study. *J Athl Train.* 2019;54(9):953-8.
- 575 [20] Jie T, Xu D, Zhang Z, Teo EC, Baker JS, Zhou H, et al. Structural and
576 Organizational Strategies of Locomotor Modules during Landing in Patients with
577 Chronic Ankle Instability. *Bioengineering (Basel).* 2024;11(5).
- 578 [21] Jildeh TR, Buckley P, Abbas MJ, Page B, Young J, Mehran N, et al. Impact of

-
- 579 Patellar Tendinopathy on Player Performance in the National Basketball
580 Association. *Orthop J Sports Med.* 2021;9(9):23259671211025305.
- 581 [22] Kerkman JN, Daffertshofer A, Gollo LL, Breakspear M, Boonstra TW. Network
582 structure of the human musculoskeletal system shapes neural interactions on
583 multiple time scales. *Sci Adv.* 2018;4(6):eaat0497.
- 584 [23] Khou SB, Saki F, Tahayori B. Muscle activation in the lower limb muscles in
585 individuals with dynamic knee valgus during single-leg and overhead squats: a
586 meta-analysis study. *BMC Musculoskeletal Disorders.* 2024;25(1):652.
- 587 [24] Kubo K, Ikebukuro T, Yata H. Effects of squat training with different depths on
588 lower limb muscle volumes. *Eur J Appl Physiol.* 2019;119(9):1933-42.
- 589 [25] Latash ML. Motor synergies and the equilibrium-point hypothesis. *Motor Control.*
590 2010;14(3):294-322.
- 591 [26] Lee DD, Seung HS. Algorithms for non-negative matrix factorization.
592 Proceedings of the 13th International Conference on Neural Information
593 Processing Systems; Denver, CO: MIT Press; 2000. p. 535–41.
- 594 [27] Li F, Song Y, Cen X, Sun D, Lu Z, Bíró I, et al. Comparative Efficacy of Vibration
595 foam Rolling and Cold Water Immersion in Amateur Basketball Players after a
596 Simulated Load of Basketball Game. *Healthcare (Basel).* 2023;11(15).
- 597 [28] Ma Y, Shi C, Xu J, Ye S, Zhou H, Zuo G. A Novel Muscle Synergy Extraction
598 Method Used for Motor Function Evaluation of Stroke Patients: A Pilot Study.
599 *Sensors (Basel).* 2021;21(11).
- 600 [29] Malliaras P, Barton CJ, Reeves ND, Langberg H. Achilles and patellar
601 tendinopathy loading programmes : a systematic review comparing clinical
602 outcomes and identifying potential mechanisms for effectiveness. *Sports Med.*
603 2013;43(4):267-86.
- 604 [30] Pietrosimone LS, Blackburn JT, Wikstrom EA, Berkoff DJ, Docking SI, Cook J,
605 et al. Differences in Biomechanical Loading Magnitude During a Landing Task in
606 Male Athletes with and without Patellar Tendinopathy. *J Athl Train.* 2021;57(11-
607 12):1062-71.
- 608 [31] Saito H, Yokoyama H, Sasaki A, Kato T, Nakazawa K. Evidence for basic units of

-
- 609 upper limb muscle synergies underlying a variety of complex human
610 manipulations. *J Neurophysiol.* 2022;127(4):958-68.
- 611 [32] Santuz A, Ekizos A, Janshen L, Mersmann F, Bohm S, Baltzopoulos V, et al.
612 Modular Control of Human Movement During Running: An Open Access Data
613 Set. *Front Physiol.* 2018;9:1509.
- 614 [33] Sawers A, Allen JL, Ting LH. Long-term training modifies the modular structure
615 and organization of walking balance control. *J Neurophysiol.* 2015;114(6):3359-
616 73.
- 617 [34] Scanlan AT, Dascombe BJ, Reaburn PR. The construct and longitudinal validity
618 of the basketball exercise simulation test. *J Strength Cond Res.* 2012;26(2):523-
619 30.
- 620 [35] Sharif F, Ahmad A, Shabbir A. Does the ultrasound imaging predict lower limb
621 tendinopathy in athletes: a systematic review. *BMC Med Imaging.* 2023;23(1):217.
- 622 [36] Tayfur A, Haque A, Salles JI, Malliaras P, Screen H, Morrissey D. Are Landing
623 Patterns in Jumping Athletes Associated with Patellar Tendinopathy? A Systematic
624 Review with Evidence Gap Map and Meta-analysis. *Sports Med.* 2022;52(1):123-
625 37.
- 626 [37] Tigrini A, Verdini F, Fioretti S, Mengarelli A. On the Decoding of Shoulder Joint
627 Intent of Motion From Transient EMG: Feature Evaluation and Classification.
628 *IEEE Transactions on Medical Robotics and Bionics.* 2023;5:1037-44.
- 629 [38] Todorov E. Optimality principles in sensorimotor control. *Nat Neurosci.*
630 2004;7(9):907-15.
- 631 [39] van der Worp H, van Ark M, Roerink S, Pepping GJ, van den Akker-Scheek I,
632 Zwerver J. Risk factors for patellar tendinopathy: a systematic review of the
633 literature. *Br J Sports Med.* 2011;45(5):446-52.
- 634 [40] Vermeulen S, De Bleecker C, Spanhove V, Segers V, Willems T, Roosen P, et al.
635 The effect of fatigue on spike jump biomechanics in view of patellar tendon
636 loading in volleyball. *Scand J Med Sci Sports.* 2023;33(11):2208-18.
- 637 [41] Vincent KR, Vasilopoulos T, Montero C, Vincent HK. Eccentric and Concentric
638 Resistance Exercise Comparison for Knee Osteoarthritis. *Med Sci Sports Exerc.*

639 2019;51(10):1977-86.

640 [42] Wang Y-X, Zhang Y. Nonnegative Matrix Factorization: A Comprehensive Review.

641 IEEE Transactions on Knowledge and Data Engineering. 2013;25:1336-53.

642 [43] Yokoyama H, Kato T, Kaneko N, Kobayashi H, Hoshino M, Kokubun T, et al.

643 Basic locomotor muscle synergies used in land walking are finely tuned during

644 underwater walking. Sci Rep. 2021;11(1):18480.

645

ACCEPTED